

# Histidine 6.55 Is a Major Determinant of Ligand-Biased Signaling in Dopamine D<sub>2L</sub> Receptor

Nuska Tschammer, Stefan Bollinger, Terry Kenakin, and Peter Gmeiner

Department of Chemistry and Pharmacy, Emil Fischer Center, Friedrich Alexander University, Erlangen, Germany (N.T., S.B., P.G.); and Department of Biological Reagents and Assay Development, GlaxoSmithKline Research and Development, Research Triangle Park, North Carolina (T.K.)

Received August 9, 2010; accepted December 16, 2010

## ABSTRACT

In our previous studies, we demonstrated that the mutation of His393<sup>6.55</sup> to alanine results in an increased affinity of 1,4-disubstituted phenylpiperazines to the dopamine D<sub>2L</sub> receptor. This change most likely accounts for the reduced steric hindrance in this part of the binding pocket. In this work, we investigated the role of the steric hindrance imposed by the residue His393<sup>6.55</sup> for the receptor activation modulated by 1,4-disubstituted aromatic piperidines/piperazines. Site-directed mutagenesis and ligand modifications were used to probe the structural basis of ligand efficacy. The operational model of agonism was used to quantify the ligand bias between the ability of compounds to inhibit cAMP accumulation and stimulate extracellular signal-regulated kinase 1/2 (ERK1/2) phosphorylation. Whereas substantial ligand-biased signaling

was observed for the D<sub>2L</sub> wild-type receptor, an overall increase in agonism was observed for the D<sub>2L</sub> H393<sup>6.55</sup>A mutant without noteworthy functional selectivity. Targeted chemical modification of the phenylpiperazine moiety at the site of its interaction with the residue His393<sup>6.55</sup> led to the functionally selective ligand {3-[4-(2,3-dihydro-benzofuran-7-yl)-piperazin-1-yl]-propyl}-pyrazol[1,5-a]pyridine-3-carboxamide (FAUC350) that has distinct signaling profiles toward adenylyl cyclase and ERK1/2. FAUC350 behaves as an antagonist in the inhibition of cAMP accumulation and as a partial agonist in the stimulation of ERK1/2 phosphorylation (efficacy = 55%). Overall, the residue His393<sup>6.55</sup> and proximate molecular substructures of receptor ligands were identified to be crucial for multidimensional ligand efficacy.

## Introduction

Because of its implication in various neurological and psychiatric disorders and as a target of antipsychotic drugs, the dopamine D<sub>2</sub> receptor is one of the most studied monoaminergic seven-transmembrane (7TM) receptors. It is well established that, similar to other 7TM receptors, D<sub>2</sub> has the ability to differentially process ligand-based signals to produce a partial activation of cellular signaling pathways in response to some ligands (Burris et al., 2002; Gay et al., 2004; Lane et al., 2007; Urban et al., 2007; Klewe et al., 2008; Masri et al., 2008). Aripiprazole, a 1,4-disubstituted phenylpiperazine, is the first D<sub>2</sub>/D<sub>3</sub> dopamine receptor drug that acts as a partial agonist and has been approved for the treatment of psychi-

atric disorders (Burris et al., 2002). The unique pharmacology of aripiprazole, a drug having both partial agonist and antagonist activity at the D<sub>2</sub> receptor, suggests that functionally selective ligands may provide a new arena for the development of novel therapeutics for psychoses and other disorders (Burris et al., 2002; Mottola et al., 2002; Klewe et al., 2008; Masri et al., 2008). However, to rationally design functionally selective drugs, structure-activity relationships for a biased signaling must be understood (Kenakin and Miller, 2010).

Previous studies on the  $\beta_2$ -adrenergic receptor documented that the activation of a 7TM receptor is a multistep process in which structurally very similar agonists and partial agonists induce distinguishable active states (Ghanouni et al., 2001; Swaminath et al., 2005). The activation of 7TM receptors encompasses the movement of transmembrane helices, in particular of TM6 in a rigid-body fashion, making vertical

Article, publication date, and citation information can be found at  
<http://molpharm.aspetjournals.org>.  
doi:10.1124/mol.110.068106.

**ABBREVIATIONS:** 7TM, seven transmembrane; TM, transmembrane domain; CHO, Chinese hamster ovary; 7-OH-DPAT, 7-hydroxy-2-(*N,N*-di-*n*-propylamino)tetralin;  $pK_{0.5}$ , negative decadic logarithm of the concentration of the compound producing 50% inhibition of the specific binding of the radioactive ligand; ERK1/2, extracellular signal-regulated kinase 1/2; ELISA, enzyme-linked immunosorbent assay; FAUC350, {3-[4-(2,3-dihydro-benzofuran-7-yl)-piperazin-1-yl]-propyl}-pyrazol[1,5-a]pyridine-3-carboxamide; FAUC335, *N*-[3-[4-(2-methylsulfanyphenyl)piperazin-1-yl]propyl]pyrazolo-[1,5-a]pyridine-3-carboxamide; FAUC321, *N*-[3-[4-(2-methoxyphenyl)piperazin-1-yl]propyl]pyrazolo-[1,5-a]pyridine-3-carboxamide; FAUC346, *N*-[4-[4-(2-methoxyphenyl)piperazin-1-yl]butyl]benzo[*b*]thiophene-2-carboxamide; CPD1, *N*-(4-(4-(2-methoxyphenyl)piperazin-1-yl)butyl)biphenyl-4-carboxamide. PBS, phosphate-buffered saline; SPD, (–)-stepholidine.

“see-saw” movements toward TM3 that result in accumulations around the main ligand-binding pocket at the extracellular side and an opening for G protein binding at the intracellular side (Elling et al., 2006; Schwartz et al., 2006; Nygaard et al., 2009; Bokoch et al., 2010).

We demonstrated that the mutation of His393<sup>6.55</sup> to alanine results in the increased affinity of 1,4-disubstituted phenylpiperazines at the D<sub>2L</sub> receptor (Ehrlich et al., 2009). We hypothesized that the additional space created by the H393<sup>6.55</sup>A mutation leads to an increase in conformational freedom of the phenylalanine residues Phe389<sup>6.51</sup> and Phe390<sup>6.52</sup>. This enables a better accommodation of the phenylpiperazine moiety to the aromatic microdomain of TM6. Molecular dynamics simulation showed that the aromatic substituent of the phenylpiperazine moiety of *N*-[3-[4-(2-methylsulfonylphenyl)piperazin-1-yl]propyl]pyrazolo-[1,5-*a*]-pyridine-3-carboxamide (FAUC335) is in close proximity to the residue His393<sup>6.55</sup>. An interaction between a ligand and His6.55 was also observed in the crystal structure of the highly homologous dopamine D<sub>3</sub> receptor (Chien et al., 2010). The steric hindrance imposed by the bulky phenylpiperazine moiety might prevent the full movement of TM6 after the binding of 1,4-disubstituted phenylpiperazine. This would lead to the reduced efficacy of these ligands, which are typically classified as antagonists or partial agonists at the D<sub>2</sub> receptor (Bettinetti et al., 2002, 2005).

To determine the importance of the residue His393<sup>6.55</sup> for receptor activation modulated by 1,4-disubstituted phenylpiperazines, we used site-directed mutagenesis and ligand

modification to reduce or enhance the steric interactions between the residue 393<sup>6.55</sup> and the phenylpiperazine moiety. We hypothesized that the reduction of the steric constraints would lead to increased efficacy, whereas the enhancement of the steric constraints would lead to decreased ligand efficacy. The D<sub>2L</sub> wild-type, D<sub>2L</sub> H393<sup>6.55</sup>A, and D<sub>2L</sub> H393<sup>6.55</sup>F receptors have been compared in their ability to bind the ligands, to inhibit the adenylyl cyclase and thus to inhibit cAMP accumulation, and to stimulate the phosphorylation of ERK1/2 after treatment with dopamine-like agonists and partial agonists from the group of 1,4-disubstituted phenylpiperazines, including the tailor-made ligand {3-[4-(2,3-dihydro-benzofuran-7-yl)-piperazin-1-yl]-propyl}-pyrazolo[1,5-*a*]pyridine-3-carboxamide (FAUC350). As a molecular indicator of differences in the mechanism of agonist action, the operational model of agonism was used to quantify the ability of an agonist to elicit a response in a given assay, calculate the bias between the signaling pathways, and calculate the bias between the wild-type and mutant receptor (Black and Leff, 1983; Kenakin, 2009; Kenakin and Miller, 2010; Evans et al., 2011).

## Materials and Methods

**Materials.** Dulbecco's modified Eagle's medium/F-12, L-glutamine, fetal bovine serum, penicillin-streptomycin, zeocin, and hygromycin B were purchased from Invitrogen (Carlsbad, CA). Pertussis toxin from *Bordetella pertussis* was purchased from Sigma (St. Louis, MO). [<sup>3</sup>H]spiperone (97 Ci/mmol) was purchased from GE Healthcare (Chalfont St. Giles, Buckinghamshire, UK). Dopamine (3,4-dihydroxyphenethylamine), quinpirole [(−)-quinpirole hydrochloride], spiperone, haloperidol, 7-hydroxy-2-(*N,N*-di-*n*-propylamino)tetralin (7-OH-DPAT),

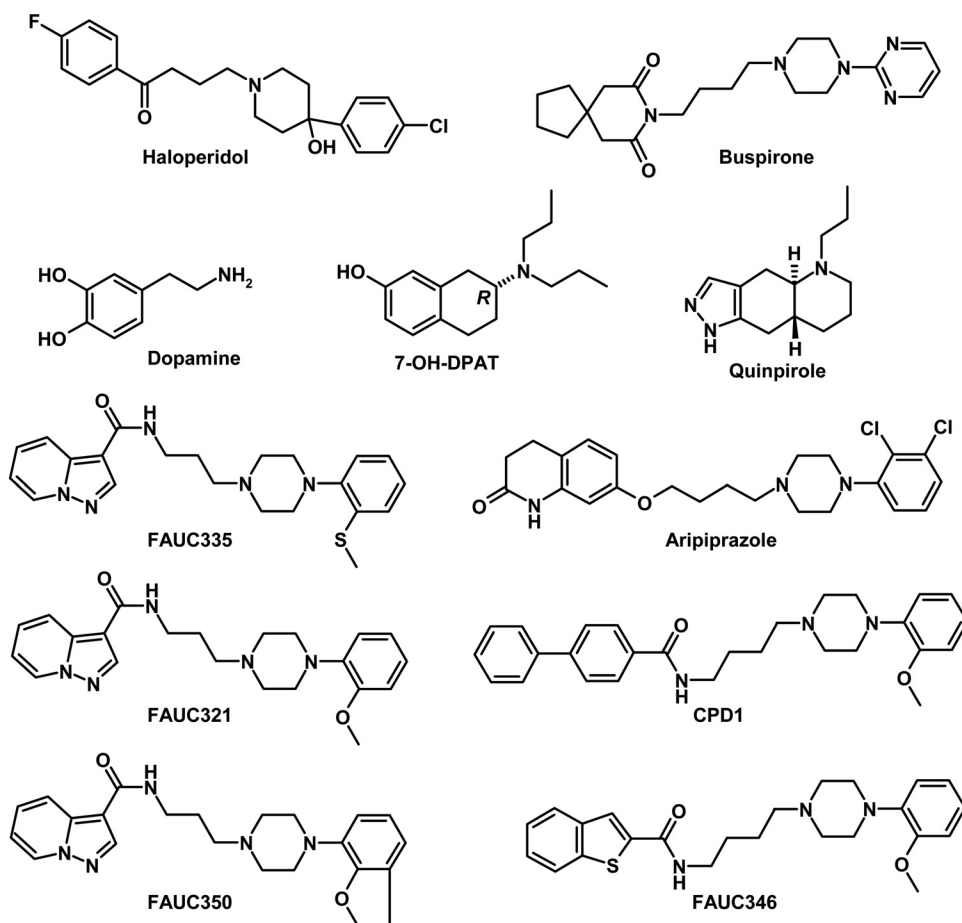


**Fig. 1.** Chemical structures of the ligands investigated in this study.

and other compounds were purchased from Sigma, unless otherwise stated. The compounds FAUC335 (Ehrlich et al., 2009), *N*-[3-[4-(2-methoxyphenyl)piperazin-1-yl]propyl]pyrazolo-[1,5-*a*]pyridine-3-carboxamide (FAUC321) (Bettinetti et al., 2002), *N*-(4-(4-(2-methoxyphenyl)piperazin-1-yl)butyl)biphenyl-4-carboxamide (CPD1) (Hackling et al., 2003), *N*-[4-[4-(2-methoxyphenyl)piperazin-1-yl]butyl]benzo[*b*]-thiophene-2-carboxamide (FAUC346) (Bettinetti et al., 2002), and aripiprazole (Oshiro et al., 1998) were synthesized as described previously. See Fig. 1 for structures.

**Chemistry.** Detailed description of the FAUC350 synthesis and the synthesis scheme are in the Supplemental Data. In general, reagents and dry solvents were obtained from commercial sources unless stated otherwise and were used as received. Reactions were conducted under dry N<sub>2</sub>. Evaporations of product solutions were done in vacuo with a rotary evaporator. Column chromatography was performed with 60 μm silica gel. For thin-layer chromatography silica gel, 60-μm plates were used (UV, I<sub>2</sub>, or ninhydrin detection). <sup>1</sup>H-NMR spectra were recorded at 360 MHz on a Bruker Avance 360 (Bruker, Milan, Italy) in CDCl<sub>3</sub> at 300 K; chemical shifts are given in δ relative to tetramethylsilane in ppm (tetramethylsilane = 0). IR spectra were measured on a Jasco (Tokyo, Japan) 410 FT-IR spectrometer. Electron impact mass spectrometry was done by electron impact ionization (70 eV) with a solid inlet on a JEOL (Tokyo, Japan) GCmate II spectrometer. High-resolution mass spectrometry was done at a resolution of M/ΔM = 5000 relative to perfluorokerosene on a JEOL GCmate II spectrometer. Purity was assessed by analytical high-performance liquid chromatography [Agilent 1100 preparative series (Agilent Technologies, Santa Clara, CA), equipped with a multiwavelength detector; column: Zorbax Eclipse XDB-C8 analytical column (Agilent Technologies), 4.6 × 150 mm, 5 μm, flow rate: 0.5 ml/min, detection wavelength: 220 nm]. System 1 (S1): 10 to 75% CH<sub>3</sub>OH in H<sub>2</sub>O + 0.1% HCO<sub>2</sub>H in 18 min; system 2 (S2): 5 to 65% CH<sub>3</sub>CN in H<sub>2</sub>O + 0.1% HCO<sub>2</sub>H in 26 min.

**Site-Directed Mutagenesis and Cloning.** The cDNA of the human dopamine D<sub>2-long</sub> (D<sub>2L</sub>) receptor was purchased from the Missouri University of Science and Technology cDNA Resource Center (Rolla, MO). The site-directed mutagenesis was performed as described previously (Ehrlich et al., 2009). The D<sub>2L</sub> wild-type, D<sub>2L</sub> H393<sup>6.55A</sup>, and D<sub>2L</sub> H393<sup>6.55F</sup> receptor cDNAs were subcloned into a pcDNA5/FRT vector (Invitrogen) using *NheI*/*XhoI* restriction sites. The entire coding region of the D<sub>2L</sub> receptor clones was sequenced to ensure that the correct mutation was introduced and to confirm the absence of unwanted mutations.

**Cell Lines and Transfection.** The Flp-in CHO cell line (Invitrogen) was maintained in Dulbecco's modified Eagle's medium/F-12 supplemented with 10% fetal bovine serum, 2 mM L-glutamine, 1% penicillin-streptomycin, and 0.25 μg/ml zeocin and kept in a humid atmosphere at 37°C with 5% CO<sub>2</sub>.

The Flp-in CHO cells were transfected with the pOG44 vector encoding Flp recombinase and the pcDNA5/FRT vector encoding specific dopamine receptors at a ratio of 9:1 using *TransIT*-LT transfection reagent (Mirus Bio Corporation, Madison, WI). Forty-eight hours after transfection, cells were subcultured and the medium was supplemented with 750 μg/ml hygromycin B to obtain colonies stably expressing dopamine receptors. For the maintenance of stably transfected cell lines, the concentration of hygromycin B was reduced to 250 μg/ml to prevent the reversion of transfected Flp-in CHO cells to a nontransfected state.

**Cell Harvest and Membrane Preparation.** Cells were washed with phosphate-buffered saline (PBS), briefly treated with Tris-EDTA buffer (10 mM Tris, 0.5 mM EDTA, 5 mM KCl, 140 mM NaCl, pH 7.4), and dissociated with a cell scraper. Cells were pelleted at 1000g for 6 min at 4°C, resuspended in Tris-EDTA-MgCl<sub>2</sub> buffer (50 mM Tris, 5 mM EDTA, 1.5 mM CaCl<sub>2</sub>, 5 mM MgCl<sub>2</sub>, 5 mM KCl, 120 mM NaCl, pH 7.4), and subsequently lysed with an Ultra-Turrax (IKA-Werke GmbH & Co. KG, Staufen, Germany). After additional centrifugation at 50,000g, the membranes were resuspended in the binding buffer (50 mM Tris, 1 mM EDTA, 5 mM MgCl<sub>2</sub>, 100 μg/ml

bacitracin, 5 μg/ml soybean trypsin inhibitor), and homogenized 10 times with a glass-Teflon homogenizer at 4°C. The homogenized membranes were shock-frozen in liquid nitrogen and stored at -80°C. The protein concentration was determined with the Lowry method with bovine serum albumin used as a standard (Lowry et al., 1951).

**Receptor Binding Studies.** Competition experiments with human D<sub>2L</sub> receptors were run with preparations of membranes from CHO cells stably expressing the corresponding receptor and [<sup>3</sup>H]spiperone at a final concentration of 0.1 to 0.2 nM. The assays were carried out with a protein concentration of 10 μg/ml and *K<sub>d</sub>* values of 0.17 ± 0.06, 0.19 ± 0.04, 0.09 ± 0.01, and 0.09 ± 0.07 nM for the D<sub>2L</sub> wild-type, D<sub>2L</sub> H393<sup>6.55A</sup>, D<sub>2L</sub> H393<sup>6.55F</sup>, and D<sub>2L</sub> H393<sup>6.55K</sup> receptors, respectively. All assays were performed in 96-well plates at a final volume of 200 μl. After incubation for 1 h at 37°C, we stopped the assay by filtration through Whatman (Clifton, NJ) GF/B filters presoaked with 0.3% polyethylenimine. The filters were rinsed five times with ice-cold Tris-NaCl buffer. After 3 h of drying at 60°C, filters were sealed with melt-on scintillator sheets MeltiLex B/HS (PerkinElmer Life and Analytical Sciences, Waltham, MA), and the filter-bound radioactivity was measured with a MicroBeta TriLux liquid scintillator counter (PerkinElmer Life and Analytical Sciences). Three to six experiments per compound were performed with each concentration in triplicate.

**Adenylyl Cyclase Inhibition Assay.** Bioluminescence-based cAMP-Glo assay (Promega, Madison, WI) was performed according to the manufacturer's instructions after adjusting the volume of required reagents for use in a white half-area 96-well plate at a final volume of 80 μl. In brief, CHO cells expressing D<sub>2L</sub> wild-type, D<sub>2L</sub> H393<sup>6.55A</sup>, or D<sub>2L</sub> H393<sup>6.55F</sup> receptor were seeded into a white half-area 96-well plate (5000 cells/well) 24 h before the assay. The cells expressed comparable amount of the receptor as determined by saturation experiments (4100 ± 750 fmol/mg for the D<sub>2L</sub> wild type, 4400 ± 350 fmol/mg for D<sub>2L</sub> H393<sup>6.55A</sup>, and 3900 ± 440 fmol/mg for D<sub>2L</sub> H393<sup>6.55F</sup>). Cells were first briefly washed with PBS, pH 7.4 to remove traces of serum and then incubated with various concentrations of substances in the presence of 20 μM forskolin in serum-free medium that contained 500 μM 3-isobutyl-1-methylxanthine and 100 μM 4-(3-butoxy-4-methoxybenzyl)imidazoline, pH 7.4. After 15 min of incubation at 25°C, the cells were lysed with cAMP-Glo lysis buffer. After lysis, the kinase reaction was performed with a reaction buffer containing protein kinase A. At the end of the kinase reaction an equal volume of Kinase-Glo reagent was added. The plates were read with a luminescence protocol on a Victor<sup>3</sup>V microplate reader (PerkinElmer Life and Analytical Sciences). The experiments were performed three to nine times per compound with each concentration in duplicate. The absolute *E<sub>max</sub>* values for quinpirole were 16,000 ± 2400, 13,700 ± 1800, and 12,800 ± 2100 relative luminescence units for the D<sub>2L</sub> wild-type, D<sub>2L</sub> H393<sup>6.55A</sup>, and D<sub>2L</sub> H393<sup>6.55F</sup>, respectively.

**PhosphoERK1/2 ELISA Assay.** The PathScan phospho-p42/44 mitogen-activated protein kinase (Thr202/Tyr204) sandwich ELISA (Cell Signaling Technology, Danvers, MA) was performed according to the manufacturer's instructions. In brief, 6 × 10<sup>6</sup> CHO cells that expressed D<sub>2L</sub> wild-type, D<sub>2L</sub> H393<sup>6.55A</sup>, or D<sub>2L</sub> H393<sup>6.55F</sup> receptor were seeded in a 100-mm plate. The cells expressed comparable amount of the receptor as determined by saturation experiments (4100 ± 750 fmol/mg for the D<sub>2L</sub> wild type, 4400 ± 350 fmol/mg for D<sub>2L</sub> H393<sup>6.55A</sup>, and 3900 ± 440 fmol/mg for D<sub>2L</sub> H393<sup>6.55F</sup>). The next day, cells were washed once with serum-free media and incubated in the presence of serum-free media for an additional 24 h. For the experiments with the pertussis toxin, 25 ng/ml toxin was added to serum-free media for 24 h. On the day of the experiment, the medium was removed and replaced with serum-free media containing various concentrations of the test substances as indicated and incubated for 5 min at 37°C. A wash with ice-cold PBS and the addition of the lysis buffer stopped the reaction. The plates were kept on ice, and cells were scraped, briefly sonicated (UP50H; Hielscher Ultrasound Technologies, Teltow, Germany), and centrifuged at 15,000g for 10 min.



The supernatant was promptly diluted with the sample diluent and incubated overnight at 4°C in the well. After intensive washing steps, the detection of the phosphorylated ERK1/2 followed. The absorbance was read at 450 nm within 2 min after addition of the STOP solution on a Victor<sup>3</sup>V microplate reader (PerkinElmer Life and Analytical Sciences). The experiment was performed three to four times per compound. The absolute  $E_{\text{max}}$  values for quinpirole were  $1.634 \pm 0.155$ ,  $1.439 \pm 0.117$ , and  $1.569 \pm 0.110$  relative absorbance units for the D<sub>2L</sub> wild-type, D<sub>2L</sub> H393<sup>6.55</sup>A, and D<sub>2L</sub> H393<sup>6.55</sup>F, respectively.

**Data Analysis.** The competition curves of the receptor binding experiments and activity assays were analyzed by nonlinear regression using the algorithms in Prism 5.0 (GraphPad Software Inc., San Diego, CA). Competition curves were fitted to the sigmoid curves by nonlinear regression analysis in which the logEC<sub>50</sub> value and the Hill coefficient were free parameters. EC<sub>50</sub> values were transformed to pK<sub>i</sub> values according to the equation of Cheng and Prusoff (1973).

Dose-response curves of the activity assays were fitted to the operational model developed by Black and Leff (1983) to obtain an estimate of the transducer constant  $\tau$ :  $E = E_m \times \tau^n / (K_A + [A])^n + \tau^n [A]^n$ , where  $E$  is the effect,  $E_m$  is the maximum possible effect,  $A$  is the agonist concentration,  $n$  is the transducer slope, and  $K_A$  is the dissociation constant of the agonist-receptor complex. The transducer constant  $\tau$  is a parameter describing the signal transduction efficiency of the system, and the intrinsic efficacy of the agonist was estimated from the fit of the data. Quinpirole was used as the full agonist reference that defines zero and a maximal (100%) response of the system. The curves of all agonists had a Hill coefficient of unity or close to unity. The log( $\tau/K_A$ ) values depicted the “strength” of a given agonist to activate a defined pathway in a defined system. Because agonists are allosteric modulators of 7TM, it is necessary that both efficacy and affinity of the agonist be captured for agonism (Kenakin, 2009; Kenakin and Miller, 2010).

The  $\Delta\log(\tau/K_A)$  values were calculated as:  $\Delta\log(\tau/K_A)_{\text{agonist/reference}} = \log(\tau/K_A)_{\text{agonist}} - \log(\tau/K_A)_{\text{reference}}$  to compare various agonists within signaling pathway. The  $\Delta\Delta\log(\tau/K_A)$  values were calculated as:  $\Delta\Delta\log(\tau/K_A)_{\text{H6.55A/wild type}} = \Delta\log(\tau/K_A)_{\text{H6.55A}} - \Delta\log(\tau/K_A)_{\text{wild type}}$ .

The  $\Delta\Delta\log(\tau/K_A)$  values provided a scale to compare various agonists between the signaling pathways or between the wild-type D<sub>2L</sub> and mutant D<sub>2L</sub> H393<sup>6.55</sup>A receptor. Detailed calculations of all parameters are summarized in Supplemental Tables 3 to 6. The calculations of 95% confidence intervals were made with the program Mathematica 5.0 and based on the algorithm described else-

where (T. Kenakin, C. Watson, V. Muniz-Medina, A. Christopoulos, S. Novick, manuscript in preparation).

Results

**Radioligand Displacement Studies.** To determine the influence of mutations H393<sup>6.55</sup>A and H393<sup>6.55</sup>F on the affinity of dopamine receptor agonists, dopamine, quinpirole, and 7-OH-DPAT were chosen. The binding data were fitted in a one-site (monophasic) and a two-site (biphasic) model. A comparison of both models revealed that the two-site (biphasic) model described the binding data for dopamine, quinpirole, and 7-OH-DPAT more accurately. For all other compounds, a one-site (monophasic) model was preferred. For the agonists, changes in the affinities at the high-affinity site will be discussed. At the D<sub>2L</sub> H393<sup>6.55</sup>A receptor, the affinity of the endogenous ligand dopamine dropped by 28-fold (Table 1). The introduction of the aromatic phenylalanine (H393<sup>6.55</sup>F) or the basic lysine (H393<sup>6.55</sup>K) did not restore the affinity of dopamine (Table 1 and Supplemental Table 1), underscoring the importance of the unique properties of the imidazole side chain of histidine for the binding of dopamine. The D<sub>2L</sub> H393<sup>6.55</sup>K mutant was expressed at approximately a 10 times lower density ( $410 \pm 120$  fmol/mg) compared with wild-type, H393<sup>6.55</sup>A, or H393<sup>6.55</sup>F receptors ( $4100 \pm 750$ ,  $4400 \pm 350$ , and  $3900 \pm 440$  fmol/mg, respectively) as determined by [<sup>3</sup>H]spiperone saturation experiments. The affinities of the synthetic dopamine receptor agonists 7-OH-DPAT and quinpirole were significantly reduced by the D<sub>2L</sub> H393<sup>6.55</sup>A mutation (12- and 63-fold, respectively). The introduction of an aromatic phenylalanine at position 6.55 (D<sub>2L</sub> H393<sup>6.55</sup>F) completely restored the affinity of 7-OH-DPAT and quinpirole completely, indicating the significance of the aromatic character of histidine for the binding affinity of these synthetic agonists.

For a range of dopamine antagonists, it was documented that the mutations D<sub>2L</sub> H393<sup>6.55</sup>L and D<sub>2L</sub> H393<sup>6.55</sup>C have only moderate compound-specific effects on the affinity of antagonists (Woodward et al., 1994; Javitch et al., 1998). The

TABLE 1  
pK<sub>i</sub> values for the dopamine receptor antagonists and agonists on D<sub>2L</sub> wild-type, D<sub>2L</sub> H393<sup>6.55</sup>A, and D<sub>2L</sub> H393<sup>6.55</sup>F receptors  
The affinities of investigated substances were determined on membrane preparations of stably transfected CHO cells expressing either D<sub>2L</sub> wild-type, D<sub>2L</sub> H393<sup>6.55</sup>A, or D<sub>2L</sub> H393<sup>6.55</sup>F receptors using [<sup>3</sup>H]spiperone displacement study. Data are derived from normalized curves of three to six experiments done in triplicate. Data were analyzed by nonlinear regression and were best-fit to one-site (monophasic) or two-site (biphasic) competition curves. pK<sub>i</sub> values were calculated according to Cheng and Prusoff (1973). The 10<sup>ΔpK<sub>i</sub>ala/wt</sup> and 10<sup>ΔpK<sub>i</sub>phe/wt</sup> values indicate the changes in the affinity. pK<sub>i</sub> values are S.E.M. Values in parentheses are Hill slope, but for pK<sub>high</sub> the values in parentheses are fraction of high-affinity sites.

| Compound     | pK <sub>i</sub> Measured | pK <sub>i</sub> for       |  |  | ΔpK <sub>i</sub> <sup>ala/wt</sup> | 10 <sup>ΔpK<sub>i</sub>ala/wt</sup> | ΔpK <sub>i</sub> <sup>phe/wt</sup> | 10 <sup>ΔpK<sub>i</sub>phe/wt</sup> |
|--------------|--------------------------|---------------------------|--|--|------------------------------------|-------------------------------------|------------------------------------|-------------------------------------|
|              |                          | D <sub>2L</sub> Wild-Type | D <sub>2L</sub> H393 <sup>6.55</sup> A | D <sub>2L</sub> H393 <sup>6.55</sup> F |                                    |                                     |                                    |                                     |
| Haloperidol  | pK <sub>0.5</sub>        | 9.41 ± 0.03 (−0.83)       | 9.60 ± 0.02 (−0.87)                    | 9.46 ± 0.03 (−0.90)                    | −0.19                              | 0.65                                | −0.05                              | 0.89                                |
|              | pK <sub>low</sub>        | 6.64 ± 0.02 (−0.85)       | 7.00 ± 0.02 (−0.91)                    | 7.70 ± 0.05 (−0.86)                    | −0.55                              | 0.28                                | −1.06                              | 0.09                                |
|              | pK <sub>high</sub>       | 8.26 ± 0.03 (−0.86)       | 8.51 ± 0.03 (−0.92)                    | 8.89 ± 0.04 (−0.98)                    | −0.25                              | 0.56                                | −0.63                              | 0.23                                |
| Buspirone    | pK <sub>0.5</sub>        | 8.85 ± 0.04 (−0.71)       | 9.35 ± 0.03 (−0.77)                    | 8.72 ± 0.03 (−0.77)                    | −0.50                              | 0.32                                | 0.13                               | 1.4                                 |
|              | pK <sub>low</sub>        | 8.43 ± 0.03 (−0.89)       | 9.11 ± 0.02 (−0.84)                    | 8.00 ± 0.04 (−0.84)                    | −0.87                              | 0.13                                | 0.43                               | 2.7                                 |
|              | pK <sub>high</sub>       | 7.41 ± 0.03 (−0.92)       | 8.30 ± 0.04 (−1.00)                    | 7.70 ± 0.04 (−0.75)                    | −0.89                              | 0.13                                | −0.29                              | 0.51                                |
| Aripiprazole | pK <sub>0.5</sub>        | 7.43 ± 0.02 (−0.70)       | 9.00 ± 0.08 (−0.64)                    | 6.89 ± 0.03 (−1.18)                    | −1.57                              | 0.03                                | 0.54                               | 3.5                                 |
|              | pK <sub>low</sub>        | 6.61 ± 0.03 (−1.02)       | 7.77 ± 0.06 (−0.88)                    | 6.76 ± 0.04 (−0.82)                    | −1.16                              | 0.07                                | −0.15                              | 0.71                                |
|              | pK <sub>high</sub>       | 6.35 ± 0.05 (−0.43)       | 5.24 ± 0.07 (−0.45)                    | 5.40 ± 0.05 (−0.41)                    | 1.11                               | 13                                  | 0.95                               | 8.9                                 |
| FAUC335      | pK <sub>0.5</sub>        | 8.08 ± 0.12 (31%)         | 6.64 ± 0.15 (36%)                      | 6.82 ± 0.10 (37%)                      | 1.44                               | 28                                  | 1.26                               | 18                                  |
|              | pK <sub>low</sub>        | 5.70 ± 0.09               | 4.52 ± 0.14                            | 4.66 ± 0.08                            | 1.18                               | 15                                  | 1.04                               | 11                                  |
|              | pK <sub>high</sub>       | 7.16 ± 0.09 (−0.40)       | 5.92 ± 0.06 (−0.51)                    | 7.05 ± 0.03 (−0.58)                    | 1.24                               | 17                                  | 0.11                               | 1.2                                 |
| FAUC321      | pK <sub>0.5</sub>        | 8.96 ± 0.06 (39%)         | 7.89 ± 0.20 (24%)                      | 8.77 ± 0.12 (26%)                      | 1.07                               | 12                                  | 0.19                               | 1.5                                 |
|              | pK <sub>low</sub>        | 6.72 ± 0.04               | 5.55 ± 0.07                            | 6.62 ± 0.04                            | 1.17                               | 15                                  | 0.10                               | 1.3                                 |
|              | pK <sub>high</sub>       | 6.21 ± 0.04 (−0.44)       | 4.96 ± 0.03 (−0.57)                    | 6.51 ± 0.03 (−0.52)                    | 1.25                               | 18                                  | −0.30                              | 0.50                                |
| FAUC350      | pK <sub>0.5</sub>        | 7.89 ± 0.12 (31%)         | 6.09 ± 0.11 (35%)                      | 7.96 ± 0.13 (31%)                      | 1.80                               | 63                                  | −0.07                              | 0.85                                |
|              | pK <sub>low</sub>        | 5.68 ± 0.08               | 4.42 ± 0.09                            | 5.96 ± 0.06                            | 1.26                               | 18                                  | −0.28                              | 0.52                                |
|              | pK <sub>high</sub>       |                           |  |  |                                    |                                     |                                    |                                     |

same was true for the affinities of the mutants we analyzed. The affinity of the antagonists haloperidol and buspirone increased moderately (up to 3.5-fold) at the D<sub>2L</sub> H393<sup>6.55</sup>A mutant. The mutation D<sub>2L</sub> H393<sup>6.55</sup>F had no influence on the affinity of haloperidol. The affinity of buspirone increased by 11-fold.

The investigated partial agonists from the group of 1,4-disubstituted phenylpiperazines can be classified by their spacer length and chemical appendage. Whereas FAUC335, FAUC321, and FAUC350 have a propylene spacer (Ehrlich et al., 2009), the homologs CPD1 (Hackling et al., 2003) and FAUC346 (Bettinetti et al., 2002) display butylene spacers between the basic center and the two-atom carboxamide moiety. Aripiprazole combines a butylene linker with a one-atom heteroaromatic ether group (Oshiro et al., 1998). The affinities of FAUC335, FAUC321, and FAUC350 gained moderately on the affinity at the D<sub>2L</sub> H393<sup>6.55</sup>A receptor (between 2.3- and 7.8-fold), and the affinities of CPD1 and FAUC346 increased 14- and 33-fold (Table 1). Aripiprazole demonstrated no significant changes in the affinity at the D<sub>2L</sub> H393<sup>6.55</sup>A receptor. At the D<sub>2L</sub> H393<sup>6.55</sup>F receptor the affinity of aripiprazole increased 4.3-fold. The affinities of other compounds remained unchanged or mildly decreased (up to 3.5-fold as for CPD1). These findings are in accordance with those of our previous study (Ehrlich et al., 2009), which demonstrated the D<sub>2L</sub> H393<sup>6.55</sup>A mutant displays an increased affinity for 1,4-disubstituted phenylpiperazines.

**Use of the Operational Model of Functional Selectivity Identified Molecule-Specific Parameters that Lead to a Ligand-Biased Signaling (Functional Selectivity).** Dose-response curves of activity assays were fitted to the operational model of agonism (Black and Leff, 1983) to obtain the dissociation constant of the agonist-receptor complex ( $K_A$ ), and an estimate of the transducer constant  $\tau$ , that describes the signal transduction efficiency of the system and the intrinsic efficacy of an agonist. Quinpirole was used as the reference full agonist and thus defines zero and a maximal (100%) response of the system. The CHO cells expressed comparable amount of receptors as determined by saturation experiments ( $4100 \pm 750$  fmol/mg for the D<sub>2L</sub> wild type,  $4400 \pm 350$  fmol/mg for D<sub>2L</sub> H393<sup>6.55</sup>A, and  $3900 \pm 440$  fmol/mg for D<sub>2L</sub> H393<sup>6.55</sup>F). The  $\log(\tau/K_A)$  values depicted the “strength” of a given agonist to activate a defined pathway in a defined system (Kenakin, 2009; Kenakin and Miller, 2010). To compare various agonists within the signaling pathways,  $\Delta\log(\tau/K_A)$  values were calculated. To compare agonists between the signaling pathways or between the wild-type and mutant receptors,  $\Delta\Delta\log(\tau/K_A)$  values were calculated. Detailed calculations of all parameters are summarized in Supplemental Tables 4 to 7.

The compounds can be partitioned into three groups based on their ability to inhibit the accumulation of cAMP (Fig. 2A). 7-OH-DPAT and dopamine had comparable  $\Delta\log(\tau/K_A)$  values (0.05 and 0.02, respectively) (Fig. 2C). The partial agonists aripiprazole, FAUC335, and FAUC321 had  $\Delta\log(\tau/K_A)$  values of  $-1.52$ ,  $-1.55$ , and  $-0.98$ , respectively, indicating their moderate ability to inhibit cAMP accumulation. FAUC346 was a very weak partial agonist with the  $\Delta\log(\tau/K_A)$  value of  $-2.50$ . FAUC350 and CPD1 were antagonists in the investigated pathway with no detectable efficacy. The calculation of the  $\Delta\log(\tau/K_A)$  was thus not possible.

G<sub>i/o</sub> protein-mediated ERK1/2 phosphorylation reached a maximum approximately 5 min after the stimulation of the D<sub>2L</sub> receptor (Fig. 2B), and it could be completely blocked by the pertussis toxin (Supplemental Fig. 1). The  $\Delta\log(\tau/K_A)$  value of dopamine was 0.21, indicating the activation profile was very similar to the reference agonist quinpirole (Fig. 2C). The ability of 7-OH-DPAT to stimulate the phosphorylation of ERK1/2 was greater than that of dopamine [ $\Delta\log(\tau/K_A)$  value 0.76]. All 1,4-disubstituted phenylpiperazines, with the exception of FAUC346, demonstrated improved  $\Delta\log(\tau/K_A)$  values, indicating their greater efficiency in modulation of the ERK1/2 phosphorylation. For FAUC350 and CPD1, which were antagonists in the cAMP pathway, the moderate ability to stimulate the ERK1/2 phosphorylation [ $\Delta\log(\tau/K_A)$  values  $-1.00$  and  $-2.57$ , respectively] was observed.

The overall bias [ $\Delta\Delta\log(\tau/K_A)$  values] of the compounds for the specific pathway modulated by the activation of the D<sub>2L</sub> wild-type receptor is depicted in Fig. 2D. Structurally very diverse molecules including dopamine, aripiprazole, and FAUC346 did not show any bias for any of these pathways. CPD1 was moderately active in the ERK1/2 pathway and behaved as an antagonist in cAMP pathway. FAUC321, which differs from FAUC335 only in a methylsulfide substituent instead of a methoxy group in position 2 of the phenylpiperazine ring (Fig. 1), showed a significant preference for the stimulation of ERK1/2 phosphorylation. The fusion of a dihydrofuran ring to the phenylpiperazine unit of FAUC350 abolished the ability of this compound to inhibit the D<sub>2L</sub> receptor mediated inhibition of cAMP accumulation (no detectable efficacy), but preserved its ability to stimulate ERK1/2 phosphorylation ( $pEC_{50}$   $7.46 \pm 0.10$ , efficacy  $55 \pm 3\%$ ) (Supplemental Data). Thus, FAUC350 represents a novel functionally selective D<sub>2L</sub> ligand with distinct signaling profiles toward adenylyl cyclase and ERK1/2. This example demonstrates that minute changes in the molecular structure suffice to modify ligand-biased signaling.

**The Mutation H393<sup>6.55</sup>A Increased the Efficacy of 1,4-Disubstituted Phenylpiperazines and Abolished the Ability of the Receptor to Recognize Biased Ligands.** To determine the influence of H393<sup>6.55</sup>A mutation on  $\Delta\log(\tau/K_A)$  and  $\Delta\Delta\log(\tau/K_A)$  values of selected compounds, the ability of the test compounds to inhibit cAMP accumulation and stimulate the ERK1/2 phosphorylation was investigated with CHO cells stably expressing the D<sub>2L</sub> H393<sup>6.55</sup>A receptor. The dose-response curves and the calculation of  $\Delta\log(\tau/K_A)$  and  $\Delta\Delta\log(\tau/K_A)$  values are depicted in Fig. 3. All 1,4-disubstituted phenylpiperazines showed substantial increase in the  $\Delta\log(\tau/K_A)$  value up to the value of 1.09 (FAUC321) in the ability to inhibit cAMP accumulation, indicating that the substitution of histidine for alanine increased the ability of 1,4-disubstituted phenylpiperazines to activate the D<sub>2L</sub> H393<sup>6.55</sup>A receptor and consequently to inhibit the cAMP accumulation. A similar effect was observed for the ability of compounds to stimulate the ERK1/2 phosphorylation. Comparing overall biases [ $\Delta\Delta\log(\tau/K_A)$  values] for the investigated pathways, 7-OH-DPAT, aripiprazole, FAUC335, FAUC321, FAUC350, and FAUC346 showed no significant bias, indicating that the substitution of the His393<sup>6.55</sup> for alanine largely abolished the ability of compounds to elicit ligand-biased signaling. The only exceptions were dopamine and CDP1. CPD1 behaved as an antagonist in the cAMP pathway at the D<sub>2L</sub> wild-type receptor and changed the pref-

erence for the signaling pathway by being more efficacious in stimulating the inhibition of cAMP accumulation than the ERK1/2 phosphorylation at the D<sub>2L</sub> H393<sup>6.55</sup>A receptor.

**The Residue His6.55 Is Crucial for Ligand Efficacy and Ligand-Biased Signaling at the D<sub>2L</sub> Receptor.** To quantify ligand-biased signaling and the bias between the

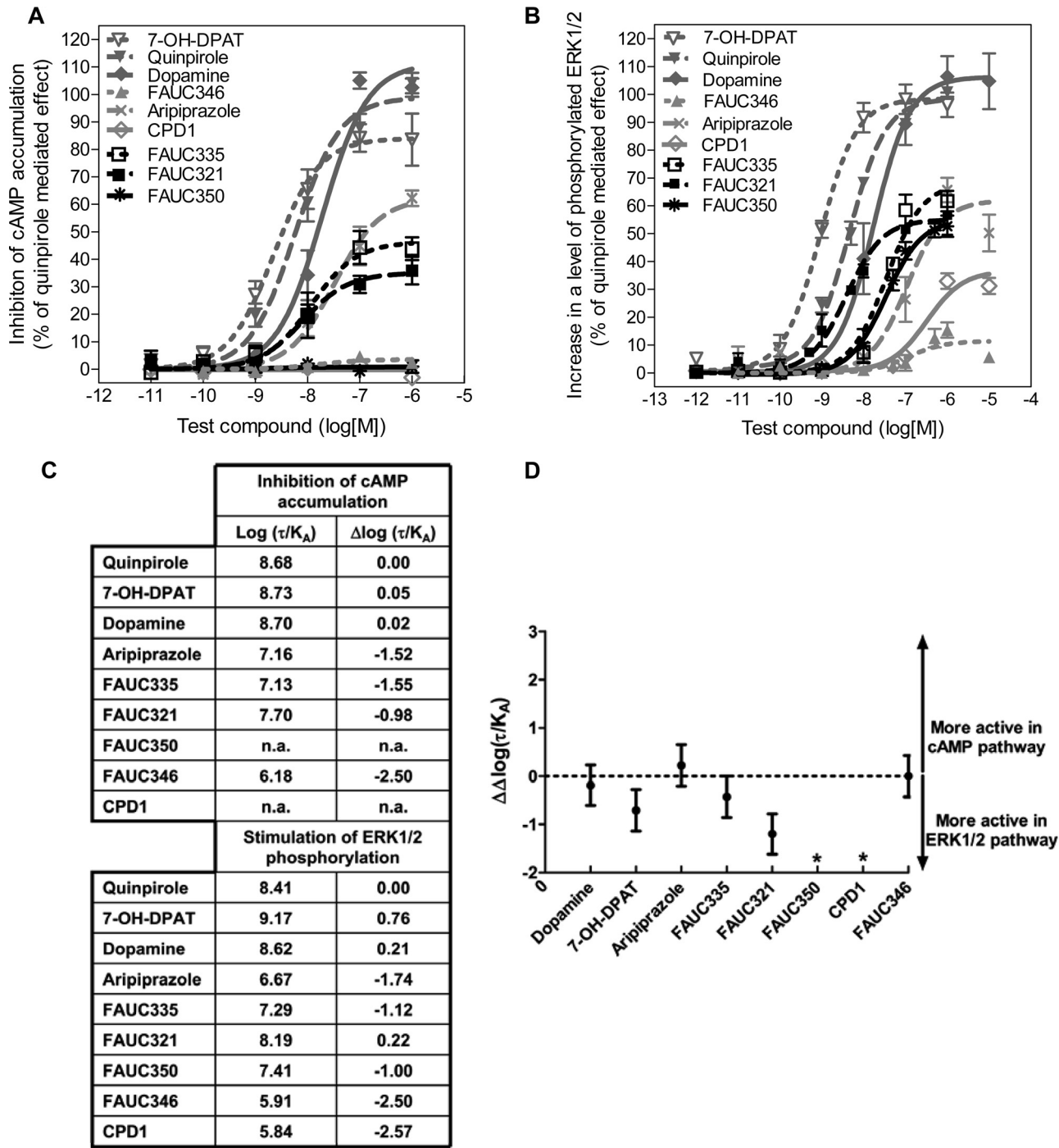


**Fig. 2.** Use of the operational model of agonism to quantify the ligand bias at the D<sub>2L</sub> wild-type receptor. The assays were performed on the D<sub>2L</sub> wild-type receptor expressing CHO cells. A, the inhibition of cAMP accumulation. The cells were incubated with 20  $\mu$ M forskolin, and the D<sub>2L</sub> wild-type receptor-mediated inhibition of cAMP accumulation was measured after stimulation with the investigated compounds. Pooled data of three to nine experiments performed in triplicate are shown as normalized curves with error bars representing the S.E.M. The pEC<sub>50</sub> values and efficacies are summarized in Supplemental Table 2. B, the stimulation of ERK1/2 phosphorylation. Serum-starved cells were stimulated with investigated compounds for 5 min at 37°C. The level of phosphorylated ERK1/2 was detected by ELISA. Pooled data of three to four experiments are shown as normalized curves with error bars representing the S.E.M. The pEC<sub>50</sub> values and efficacies are summarized in Supplemental Table 3. C, the log( $\tau/K_A$ ) and  $\Delta\log(\tau/K_A)$  values obtained with the operational model of agonism. n.a. indicates not available because of the antagonistic behavior of the compound in the selected signaling pathway. D, the  $\Delta\Delta\log(\tau/K_A)$  values as a measure of ligand bias between the pathways. The error bar represents 95% confidence interval. When the range includes zero, the ligands are not biased with the respect to the reference agonist. \* indicates the exclusive preference of the compound for the selected signaling pathway. Detailed calculations of  $\Delta\log(\tau/K_A)$ ,  $\Delta\Delta\log(\tau/K_A)$  values, and their 95% confidence intervals are summarized in Supplemental Table 4.



D<sub>2L</sub> wild-type and the D<sub>2L</sub> H393<sup>6.55</sup>A receptors in the selected pathway, the  $\Delta\log(\tau/K_A)$  values from Figs. 2C and 3C were used for the calculation of the  $\Delta\Delta\log(\tau/K_A)$  values (describing bias) of compounds for the mutant receptor. The

analysis revealed significant bias of compounds for the mutant receptor. All compounds with the exception of dopamine were able to elicit greater response at the D<sub>2L</sub> H393<sup>6.55</sup>A receptor measured as the inhibition of cAMP accumulation

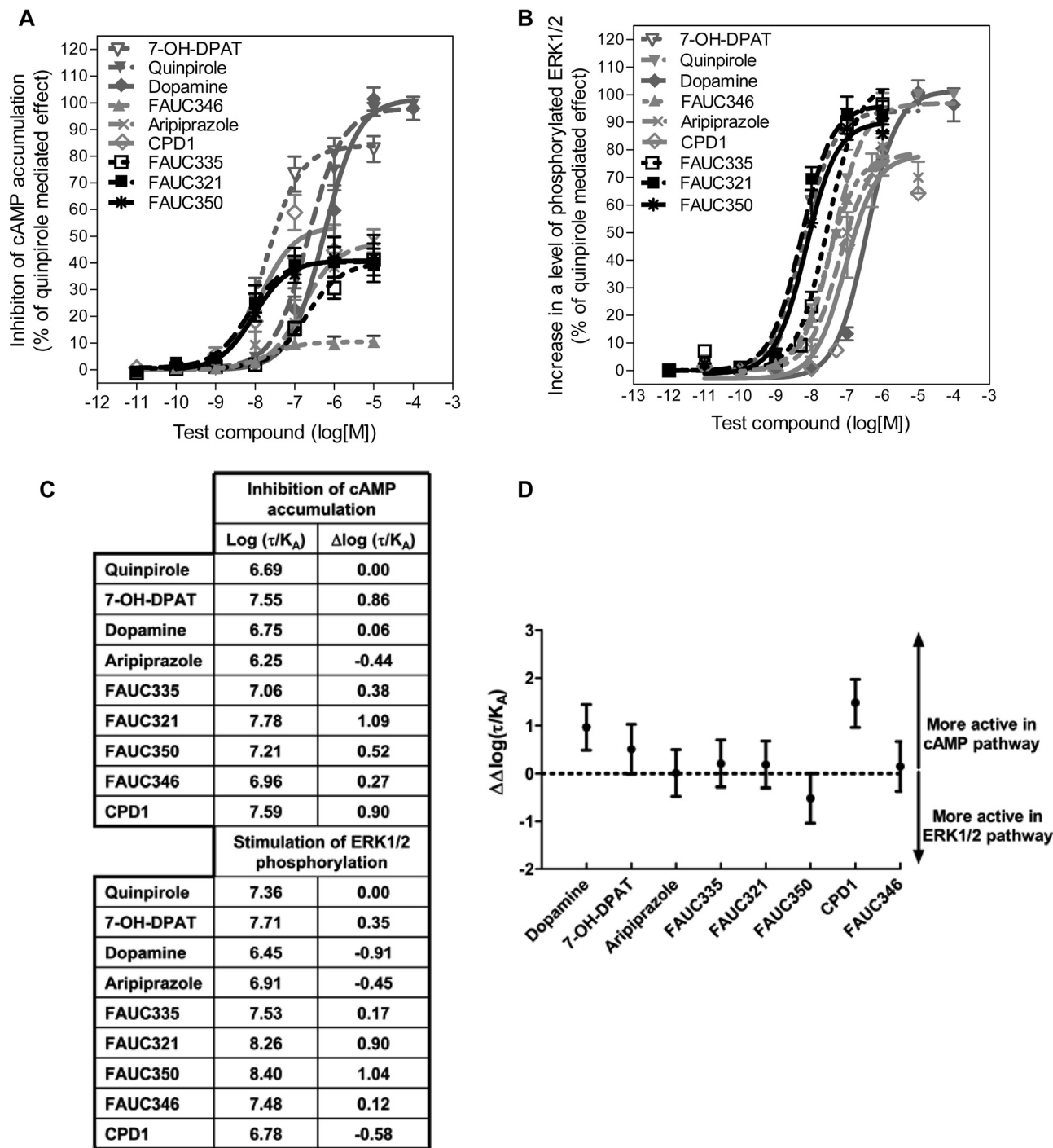


**Fig. 3.** Use of the operational model of agonism to quantify the ligand bias at the D<sub>2L</sub> H393<sup>6.55</sup>A receptor. The assays were performed on the D<sub>2L</sub> H393<sup>6.55</sup>A receptor expressing CHO cells. A, the inhibition of cAMP accumulation. The cells were incubated with 20  $\mu$ M forskolin, and the D<sub>2L</sub> H393<sup>6.55</sup>A receptor-mediated inhibition of cAMP accumulation was measured after stimulation with the investigated compounds. Pooled data of three to nine experiments performed in triplicate are shown as normalized curves with error bars representing the S.E.M. The pEC<sub>50</sub> values and efficacies are summarized in Supplemental Table 2. B, the stimulation of ERK1/2 phosphorylation. Serum-starved cells were stimulated with the investigated compounds for 5 min at 37°C. The level of phosphorylated ERK1/2 was detected by ELISA. Pooled data of three to four experiments are shown as normalized curves with error bars representing the S.E.M. The pEC<sub>50</sub> values and the efficacies are summarized in Supplemental Table 3. C, the  $\log(\tau/K_A)$  and  $\Delta\log(\tau/K_A)$  values obtained with the operational model of agonism. D, the  $\Delta\Delta\log(\tau/K_A)$  values as a measure of ligand bias between the pathways. The error bars represent 95% confidence interval. When the range includes zero, the ligands are not biased with respect to each other. \* indicates exclusive preference of the compound for the selected signaling pathway. Detailed calculations of  $\Delta\log(\tau/K_A)$ ,  $\Delta\Delta\log(\tau/K_A)$  values, and their 95% confidence intervals are summarized in Supplemental Table 5.

(Fig. 4A). Dopamine did not discriminate between the  $D_{2L}$  H393<sup>6.55</sup>A and  $D_{2L}$  wild-type receptors in this assay. The ability of 1,4-disubstituted phenylpiperazines to stimulate the phosphorylation of ERK1/2 was strongly biased for the  $D_{2L}$  H393<sup>6.55</sup>A receptor (Fig. 4B). Dopamine and 7-OH-DPAT were more active at the  $D_{2L}$  wild-type receptor (Fig. 4B), which is in accordance with their greater binding affinity on this receptor (Table 1). This overall increase in the activity of 1,4-disubstituted phenylpiperazines at the  $D_{2L}$  H393<sup>6.55</sup>A receptor implied that the introduction of a smaller alanine at position 393<sup>6.55</sup> facilitates the movement of TM6 upon ligand binding; this results in the increased efficacy of 1,4-disubstituted phenylpiperazines. Consequently, we anticipated that an introduction of a slightly bulkier residue at the position 393<sup>6.55</sup> should negatively influence the efficacy of 1,4-disubstituted phenylpiperazines compared with the  $D_{2L}$  wild-type receptor. The steric hindrance imposed by the slightly bulkier residue would prevent the full movement of TM6 upon

binding of 1,4-disubstituted phenylpiperazines and consequently lead to a reduced efficacy of these compounds.

To prove this hypothesis, the investigated compounds were tested on  $D_{2L}$  H393<sup>6.55</sup>F receptor-expressing CHO cells by measuring the inhibition of cAMP accumulation and the stimulation of ERK1/2 phosphorylation. The results obtained from measurements of the inhibition of cAMP accumulation supported our hypothesis. The standard dopamine receptor agonists quinpirole, 7-OH-DPAT, and dopamine preserved their agonist nature also at the  $D_{2L}$  H393<sup>6.55</sup>F receptor (Fig. 5A). The ability of 1,4-disubstituted phenylpiperazines to mediate the inhibition of cAMP accumulation was significantly reduced. FAUC350 and FAUC335 were weak partial agonists and aripiprazole and FAUC321 were weak inverse agonists, whereas FAUC346 and CPD1 acted as very strong inverse agonists. The mutation H393<sup>6.55</sup>F considerably reduced the efficacy of 1,4-disubstituted phenylpiperazines.

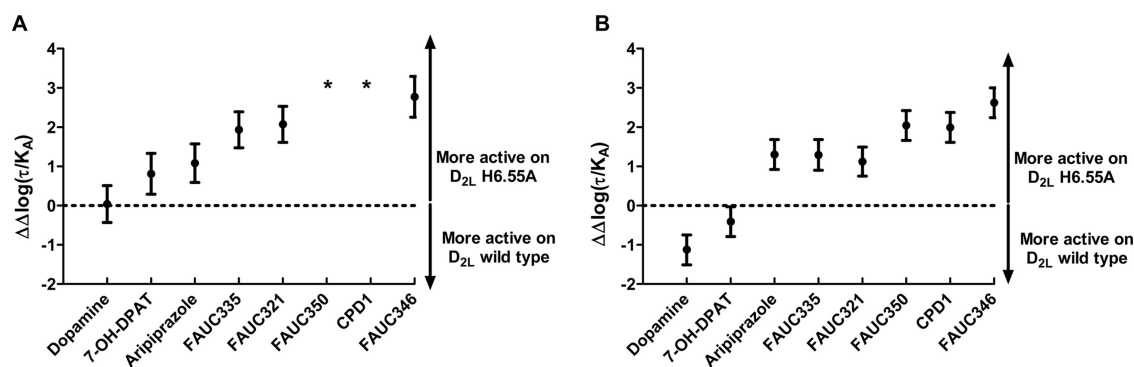


**Fig. 4.** Use of the operational model of agonism to quantify the ligand bias among the  $D_{2L}$  wild-type and  $D_{2L}$  H393<sup>6.55</sup>A receptors. The  $\Delta\log(\tau/K_A)$  values from Figs. 2C and 3C were used to calculate the  $\Delta\Delta\log(\tau/K_A)$  values as a measure of ligand bias between the  $D_{2L}$  wild-type and  $D_{2L}$  H393<sup>6.55</sup>A receptors. The error bars represent 95% confidence interval. When the range includes zero, the ligands are not biased with respect to each other. \* indicates exclusive preference of the compound for the selected signaling pathway. Detailed calculations of  $\Delta\log(\tau/K_A)$ ,  $\Delta\Delta\log(\tau/K_A)$  values, and their 95% confidence intervals are summarized in Supplemental Table 6 and 7. A, the  $\Delta\Delta\log(\tau/K_A)$  values as a measure of ligand bias between the  $D_{2L}$  wild-type and  $D_{2L}$  H393<sup>6.55</sup>A receptors in their ability to inhibit cAMP accumulation. B, the  $\Delta\Delta\log(\tau/K_A)$  values as a measure of ligand bias between the  $D_{2L}$  wild-type and  $D_{2L}$  H393<sup>6.55</sup>A receptors in their ability to stimulate ERK1/2 phosphorylation.

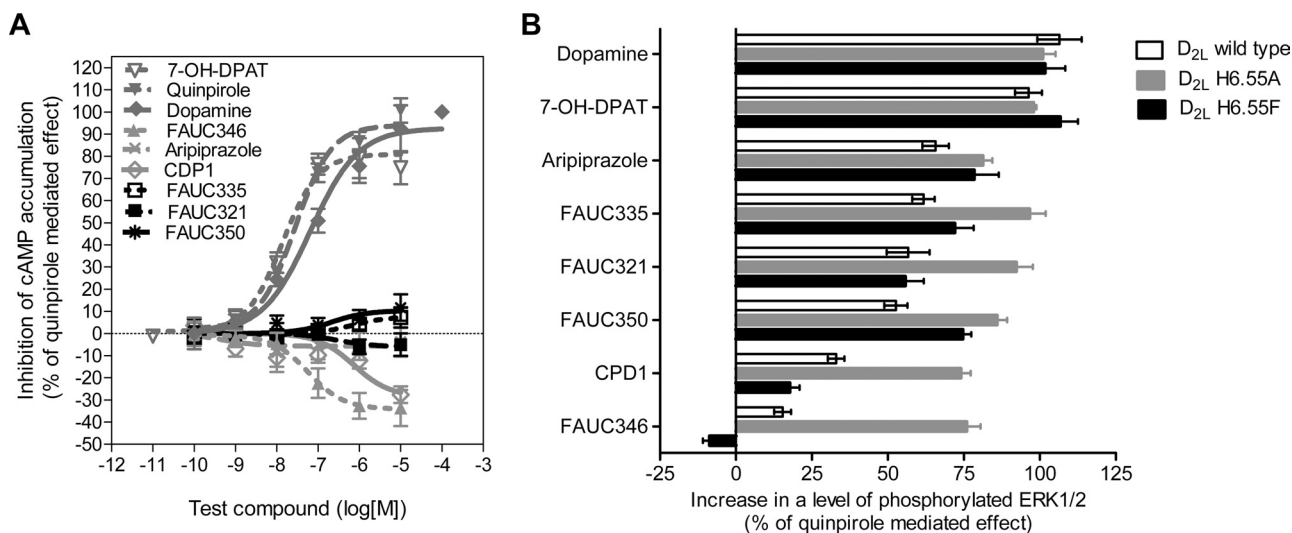


**Fig. 5.** The ability of investigated compounds to activate the  $D_{2L}$  H393<sup>6.55</sup>F receptor. A, the inhibition of cAMP accumulation. The cells were incubated with 20  $\mu$ M forskolin, and the  $D_{2L}$  H393<sup>6.55</sup>F receptor-mediated inhibition of cAMP accumulation was measured after stimulation with the investigated compounds. Pooled data of three to four experiments performed in triplicate are shown as normalized curves with error bars representing the S.E.M. B, the stimulation of ERK1/2 phosphorylation. Serum-starved cells were stimulated with discrete concentration of investigated compounds for 5 min at 37°C. Dopamine, 7-OH-DPAT, and quinpirole were tested at 10  $\mu$ M, and aripiprazole, FAUC335, FAUC321, FAUC350, FAUC346, and CPD1 were tested at 1  $\mu$ M. The level of phosphorylated ERK1/2 was detected by ELISA. The mean values with error bars representing the S.E.M. of three to four experiments are shown.



To estimate the ability of the investigated compounds to stimulate D<sub>2L</sub> H393<sup>6.55</sup>F receptor-mediated phosphorylation of ERK1/2, we used discrete sample concentrations (between 1 and 10  $\mu$ M). As expected, the mutation H393<sup>6.55</sup>F had no influence on the efficacy of dopamine and 7-OH-DPAT (Fig. 5B). We were surprised to find that the mutation H393<sup>6.55</sup>F had no influence on the efficacy of FAUC335 and FAUC321 and only a minor effect on FAUC350 and CDP1. Only FAUC346 reacted on the mutation H393<sup>6.55</sup>F with an attenuation of efficacy (from 15% at the D<sub>2L</sub> wild-type to -8% at the D<sub>2L</sub> H393<sup>6.55</sup>F receptor). These observations underscore the role of His393<sup>6.55</sup> in the D<sub>2L</sub> receptor as a crucial determinant of multidimensional ligand efficacy.

## Discussion

The ability of the D<sub>2L</sub> receptor to differentially process ligand-biased signals to produce limited activation of downstream signaling pathways in response to some ligands is well documented (Burris et al., 2002; Gay et al., 2004; Lane et al., 2007; Urban et al., 2007; Klewe et al., 2008). Dihydropyridine was the first ligand reported that displayed a functionally selective profile when fully inhibiting cAMP accumulation, but it was not able to inhibit the synthesis and release of dopamine or inhibit the firing of nigral dopaminergic neurons (Mottola et al., 2002). Functional selectivity was also reported for propylnorapomorphine, dinapsoline, and (*S*)-(-)-3-(3-hydroxyphenyl)-*N*-propylpiperidine (Gay et al., 2004; Lane et al., 2007). The best example of functional selectivity at the D<sub>2</sub> receptor is aripiprazole, an approved drug for the treatment of psychiatric disorders; it is able to partially activate the G proteins but unable to stimulate  $\beta_2$ -arrestin recruitment (Burris et al., 2002; Urban et al., 2007; Klewe et al., 2008; Masri et al., 2008). Functionally selective ligands may thus provide important tools for the treatment of various disorders.

Despite the great progress in the understanding of 7TM receptor activation, the structure-activity relationships of biased signaling (or functional selectivity) are still inadequately understood. With the combination of medicinal chemistry and the methods of molecular biology, we tried to increase the understanding of the D<sub>2L</sub> receptor activation with the emphasis on the elucidation of tailor-made ligands and site-directed receptor modifications needed to tune the functional selectivity or ligand bias. The foundation of our present work is built on the observation that a subtle modification of one amino acid in TM6 of the D<sub>2L</sub> receptor, a region that is critical for ligand binding and receptor activation, can elicit changes in the signaling properties as we reported for the RASSL (Receptor Activated Solely by Synthetic Ligands) D<sub>2L</sub> F390<sup>6.52</sup>W (Tschammer et al., 2010). The mutation of His393<sup>6.55</sup>, which is conserved within the D<sub>2</sub>-like dopamine receptors, led to an increase in the affinity of 1,4-disubstituted phenylpiperazines to the H393<sup>6.55</sup>A receptor (Ehrlich et al., 2009). To further explore this increase in affinity at the D<sub>2L</sub> H393<sup>6.55</sup>A receptor, the ability of 1,4-disubstituted phenylpiperazines to produce the response the D<sub>2L</sub> wild-type, D<sub>2L</sub> H393<sup>6.55</sup>A, and D<sub>2L</sub> H393<sup>6.55</sup>F receptors was investigated in whole-cell assays, and the inhibition of adenylyl cyclase and the stimulation of ERK1/2 phosphorylation were measured. Distinct signaling profiles toward adenylyl cyclase and ERK1/2 were previously reported for  $\beta_1$  and  $\beta_2$  ligands (Galandrin and Bouvier, 2006). Our data were subjected to

the operational model of agonism (Black and Leff, 1983) that was applied to calculate the agonist bias.

Because the agonist bias must be described in terms of both affinity and efficacy (Kenakin, 2009; Kenakin and Miller, 2010; Evans et al., 2011), use of the operational model of agonism enabled us to quantify the bias of a ligand for a selected signaling pathway. The affinity, denoted as  $K_A$ , describes the equilibrium dissociation constant of the agonist-receptor complex, and transduction constant, denoted as  $\tau$ , is a parameter encompassing both the efficacy of the agonist and the sensitivity of a system. The value of  $\Delta\log(\tau/K_A)$ , relative to a chosen standard for the system quantifies the relative ability of each agonist to produce a response. The difference of the  $\Delta\log(\tau/K_A)$  between selected pathways yields  $\Delta\Delta\log(\tau/K_A)$ , which describes agonist bias or functional selectivity of the ligand.

Use of the operational model of functional selectivity identified molecule-specific parameters essential for fine-tuning of functional selectivity at the D<sub>2L</sub> receptor. Within the dopamine-simulating recognition element of the ligand, substitution of the methylsulfide group (FAUC335) for the methoxy group (FAUC321) increased the preference for the stimulation of ERK1/2 phosphorylation. The substitution of the methoxy group (FAUC321) for a more sterically demanding dihydrofuran ring (FAUC350) increased the bias of the compound for the ERK1/2 pathway even further and completely abolished the ability of FAUC350 to stimulate the inhibition of cAMP accumulation. This observation underscores the importance of minor structural changes to induce functional selectivity. In fact, FAUC350 displayed distinct signaling profiles toward adenylyl cyclase and ERK1/2. FAUC350 behaved as an antagonist in the inhibition of cAMP accumulation and as a partial agonist in the stimulation of ERK1/2 phosphorylation (efficacy = 55%). According to our molecular dynamics simulation, the aromatic substituent of the phenylpiperazine moiety of FAUC335 is in close proximity to the residue His393<sup>6.55</sup> of the D<sub>2</sub> receptor (Ehrlich et al., 2009). The latest crystal structure of the highly homologous dopamine D<sub>3</sub> receptor cocrystallized with eticlopride confirmed the interactions between the ligand and His6.55 (Chien et al., 2010).

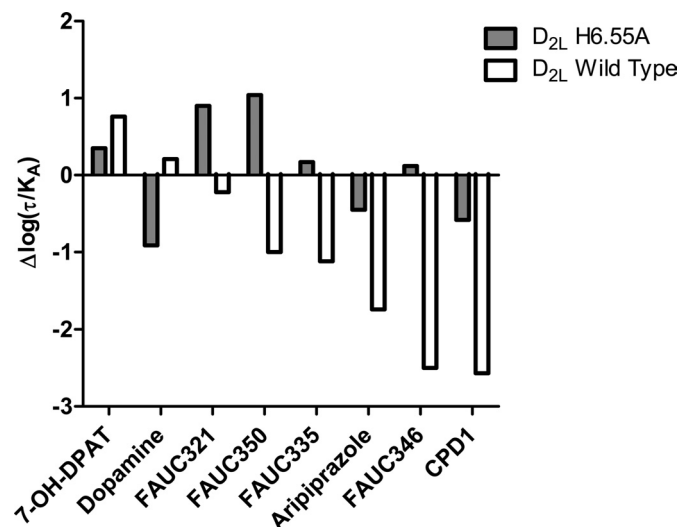


**Fig. 6.** The D<sub>2L</sub> H393<sup>6.55</sup>A mutant tends to be more readily activated by various agonists. The diagram is based on the data obtained for the stimulation of ERK1/2 phosphorylation by D<sub>2L</sub> wild type and D<sub>2L</sub> H393<sup>6.55</sup>A (Figs. 2 and 3 and Supplemental Table 7).

The residue at position 6.55 was postulated to be an important structural determinant for differentiating the pharmacological dual specificities of (–)-stepholidine (SPD) for D<sub>1</sub> and D<sub>2</sub> receptors; SPD operated as an agonist at D<sub>1</sub> and as an antagonist at D<sub>2</sub> (Jin et al., 2002; Fu et al., 2007). In the D<sub>1</sub> receptor, position 6.55 is occupied by Asn292<sup>6.55</sup>. Mutation of the similarly positioned His297<sup>6.52</sup> in  $\mu$ -opioid receptor to asparagine enhanced the intrinsic activity of the alkaloid partial agonists, thus identifying a discrete region of the receptor critical for determination of the receptor activation by a specific pharmacophore (Spivak et al., 1997). For the  $\beta_2$ -adrenergic receptor, the inward movement of TM6 permits the interaction of Asn293<sup>6.55</sup> with agonists and changes the receptor to an active conformation (Wieland et al., 1996; Zuurmond et al., 1999; Bokoch et al., 2010). The increased space in the upper binding pocket would allow an enhanced inward movement of TM6 (Schwartz et al., 2006). The space-generating substitution of His363<sup>6.55</sup> for alanine in the D<sub>2L</sub> receptor enabled the increased affinity of 1,4-disubstituted phenylpiperazines and the bias toward agonism. Similar observations have been described for mutations of the ghrelin receptor in the upper part of the binding pocket (Holst et al., 2007). Likewise, subtle changes in the structure of the ligand or the receptor at the site between TM3, TM5, and TM6 can switch the complement fragment 5a anaphylatoxin receptor on or off (Buck and Wells, 2005). As depicted in Fig. 6, which presents our data in terms of decreasing power to induce response [decreasing values of  $\Delta\log(\pi/K_A)$ ] for the wild-type versus the mutant receptor, the precipitous drop-off in agonism goes away and the mutant tends to be more or less homogeneously activated by all of the agonists; these types of mutations add a measure of permissivity to agonism.

The substitution of His363<sup>6.55</sup> for the sterically more demanding phenylalanine caused a moderate drop in the binding affinity and induced the bias of 1,4-disubstituted phenylpiperazines toward antagonism/inverse agonism; this activity was most pronounced in the inhibition of cAMP accumulation. It was proposed that inverse agonists of the  $\beta_2$ -adrenergic receptor may function in part by blocking the motion of TM6 (Bokoch et al., 2010). Similar behavior was predicted for the antagonizing properties of SPD at the D<sub>2L</sub> receptor (Fu et al., 2007).

The ability of 1,4-disubstituted phenylpiperazines to stimulate D<sub>2L</sub> H393<sup>6.55</sup>F-mediated ERK1/2 phosphorylation was not impaired, with the exception of FAUC346 that behaved as a weak inverse agonist in the ERK1/2 pathway. Typically, the activation of dopamine D<sub>2</sub> receptors liberates the G $\alpha$  subunit of the G<sub>i/o</sub> class of G proteins that leads to the inhibition of the adenylyl cyclase by the G $\alpha_i$  subunit and thus reduction of cAMP production. The liberated G $\beta\gamma$  subunit stimulates phospholipase C-induced increase in intracellular calcium that ultimately leads to downstream activation (i.e., phosphorylation) of ERK1/2 (Choi et al., 1999; Yan et al., 1999). The G $\alpha_o$  subunit does not inhibit the adenylyl cyclase (Wong et al., 1992) but itself initiates the signaling cascade resulting in ERK1/2 phosphorylation (Antonelli et al., 2000). It was reported that different agonists are able to stabilize different conformations of the receptor with different affinities for the G proteins (G<sub>o</sub> versus G<sub>i2</sub>) (Cordeaux et al., 2001; Lane et al., 2007). These distinct active states with the altered G protein coupling specificity may lead to different functional outcomes, as indirectly observed in our experi-

ments. To determine to which extent 1,4-disubstituted phenylpiperazines and the D<sub>2L</sub> His363<sup>6.55</sup> receptor mutants alter G protein coupling will require further studies.

Our observations at the D<sub>2L</sub> receptor mutants D<sub>2L</sub> H393<sup>6.55</sup>A and D<sub>2L</sub> H363<sup>6.55</sup>F contribute additional pieces of information to the understanding of D<sub>2L</sub> receptor activation and the structure-activity relationships for functional selectivity. In fact, minor ligand or receptor modifications are enough to fine-tune the ligand bias, especially when they are in close proximity to position 6.55 of the receptor. Thus, residue His393<sup>6.55</sup> and molecular substructures of receptor ligands were identified as crucial determinants of multidimensional ligand efficacy. Our investigations led to the novel functionally selective D<sub>2L</sub> ligand FAUC350, which behaves as an antagonist in the inhibition of cAMP accumulation and as a partial agonist in the stimulation of ERK1/2 phosphorylation (efficacy = 55%).

Structurally diverse compounds often do not cause any ligand-biased signaling. On the other hand, structurally similar compounds might cause ligand biased signaling as we described for the group of 1,4-disubstituted phenylpiperazines. It is not possible to foresee biased signaling solely from the structural characteristics of a ligand. We propose that once a biased ligand is identified, one can tune the degree of bias with minor structural modifications. Modifying the site of the ligand participating in the interactions with the residue in position 6.55 (His 393<sup>6.55</sup>) of the D<sub>2</sub> receptor, which is involved in receptor activation, will increase the success rate in designing desired biased ligands.

#### Acknowledgments

We thank Dr. Armin Tschammer for assisting with the software Mathematica 5.0, Dr. Ronald Altig for editing the manuscript, and two conscientious reviewers for suggesting improvements to the manuscript.

#### Authorship Contributions

*Participated in research design:* Tschammer and Gmeiner.  
*Conducted experiments:* Tschammer and Bollinger.  
*Contributed new reagents or analytic tools:* Bollinger.  
*Performed data analysis:* Tschammer, Kenakin, and Gmeiner.  
*Wrote or contributed to the writing of the manuscript:* Tschammer, Kenakin, and Gmeiner.

#### References

- Antonelli V, Bernasconi F, Wong YH, and Vallar L (2000) Activation of B-Raf and regulation of the mitogen-activated protein kinase pathway by the G $\alpha$  chain. *Mol Biol Cell* 11:1129–1142.
- Bettinetti L, Löber S, Hübner H, and Gmeiner P (2005) Parallel synthesis and biological screening of dopamine receptor ligands taking advantage of a click chemistry based BAL linker. *J Comb Chem* 7:309–316.
- Bettinetti L, Schlöter K, Hübner H, and Gmeiner P (2002) Interactive SAR studies: rational discovery of super-potent and highly selective dopamine D3 receptor antagonists and partial agonists. *J Med Chem* 45:4594–4597.
- Black JW and Leff P (1983) Operational models of pharmacological agonism. *Proc R Soc Lond B Biol Sci* 220:141–162.
- Bokoch MP, Zou Y, Rasmussen SG, Liu CW, Nygaard R, Rosenbaum DM, Fung JJ, Choi HJ, Thian FS, Kobilka TS, Puglisi JD, Weis WI, Pardo L, Prosser RS, Mueller L, and Kobilka BK (2010) Ligand-specific regulation of the extracellular surface of a G-protein-coupled receptor. *Nature* 463:108–112.
- Buck E and Wells JA (2005) Disulfide trapping to localize small-molecule agonists and antagonists for a G protein-coupled receptor. *Proc Natl Acad Sci USA* 102:2719–2724.
- Burris KD, Molski TF, Xu C, Ryan E, Tottori K, Kikuchi T, Yocca FD, and Molinoff PB (2002) Aripiprazole, a novel antipsychotic, is a high-affinity partial agonist at human dopamine D2 receptors. *J Pharmacol Exp Ther* 302:381–389.
- Cheng Y and Prusoff WH (1973) Relationship between the inhibition constant (K<sub>i</sub>) and the concentration of inhibitor which causes 50 per cent inhibition (I<sub>50</sub>) of an enzymatic reaction. *Biochem Pharmacol* 22:3099–3108.
- Chien EY, Liu W, Zhao Q, Katritch V, Han GW, Hanson MA, Shi L, Newman AH,

- Javitch JA, Cherezov V, and Stevens RC (2010) Structure of the human dopamine D3 receptor in complex with a D2/D3 selective antagonist. *Science* **330**:1091–1095.
- Choi EY, Jeong D, Park KW, and Baik JH (1999) G protein-mediated mitogen-activated protein kinase activation by two dopamine D2 receptors. *Biochem Biophys Res Commun* **256**:33–40.
- Cordeaux Y, Nickolls SA, Flood LA, Graber SG, and Strange PG (2001) Agonist regulation of D2 dopamine receptor/G protein interaction. Evidence for agonist selection of G protein subtype. *J Biol Chem* **276**:28667–28675.
- Ehrlich K, Götz A, Bollinger S, Tschammer N, Bettinetti L, Härterich S, Hübner H, Lanig H, and Gmeiner P (2009) Dopamine D2, D3, and D4 selective phenylpiperazines as molecular probes to explore the origins of subtype specific receptor binding. *J Med Chem* **52**:4923–4935.
- Elling CE, Frimurer TM, Gerlach LO, Jorgensen R, Holst B, and Schwartz TW (2006) Metal ion site engineering indicates a global toggle switch model for seven-transmembrane receptor activation. *J Biol Chem* **281**:17337–17346.
- Evans BA, Broxton N, Merlin J, Sato M, Hutchinson DS, Christopoulos A, and Summers RJ (2011) Quantification of functional selectivity at the human  $\alpha$ 1A-adrenoceptor. *Mol Pharmacol* **79**:298–307.
- Fu W, Shen J, Luo X, Zhu W, Cheng J, Yu K, Briggs JM, Jin G, Chen K, and Jiang H (2007) Dopamine D1 receptor agonist and D2 receptor antagonist effects of the natural product (–)-stepholidine: molecular modeling and dynamics simulations. *Biophys J* **93**:1431–1441.
- Galandrin S and Bouvier M (2006) Distinct signaling profiles of  $\beta$ 1 and  $\beta$ 2 adrenergic receptor ligands toward adenylyl cyclase and mitogen-activated protein kinase reveals the pluridimensionality of efficacy. *Mol Pharmacol* **70**:1575–1584.
- Gay EA, Urban JD, Nichols DE, Oxford GS, and Mailman RB (2004) Functional selectivity of D2 receptor ligands in a Chinese hamster ovary hD2L cell line: evidence for induction of ligand-specific receptor states. *Mol Pharmacol* **66**:97–105.
- Ghanouni P, Gryczynski Z, Steenhuis JJ, Lee TW, Farrens DL, Lakowicz JR, and Kobilka BK (2001) Functionally different agonists induce distinct conformations in the G protein coupling domain of the  $\beta$ 2 adrenergic receptor. *J Biol Chem* **276**:24433–24436.
- Hackling A, Ghosh R, Perachon S, Mann A, Hölte HD, Wermuth CG, Schwartz JC, Sippl W, Sokoloff P, and Stark H (2003) *N*-( $\omega$ -(4-(2-Methoxyphenyl)piperazin-1-yl)alkyl)carboxamides as dopamine D2 and D3 receptor ligands. *J Med Chem* **46**:3883–3899.
- Holst B, Mokrosinski J, Lang M, Brandt E, Nygaard R, Frimurer TM, Beck-Sickinge AG, and Schwartz TW (2007) Identification of an efficacy switch region in the ghrelin receptor responsible for interchange between agonism and inverse agonism. *J Biol Chem* **282**:15799–15811.
- Javitch JA, Ballesteros JA, Weinstein H, and Chen J (1998) A cluster of aromatic residues in the sixth membrane-spanning segment of the dopamine D2 receptor is accessible in the binding-site crevice. *Biochemistry* **37**:998–1006.
- Jin GZ, Zhu ZT, and Fu Y (2002) (–)-Stepholidine: a potential novel antipsychotic drug with dual D1 receptor agonist and D2 receptor antagonist actions. *Trends Pharmacol Sci* **23**:4–7.
- Kenakin T and Miller LJ (2010) Seven transmembrane receptors as shapeshifting proteins: the impact of allosteric modulation and functional selectivity on new drug discovery. *Pharmacol Rev* **62**:265–304.
- Kenakin TP (2009) 7TM receptor allostery: putting numbers to shapeshifting proteins. *Trends Pharmacol Sci* **30**:460–469.
- Klewe IV, Nielsen SM, Tarpø L, Urizar E, Dipace C, Javitch JA, Gether U, Egebjerg J, and Christensen KV (2008) Recruitment of  $\beta$ -arrestin2 to the dopamine D2 receptor: insights into anti-psychotic and anti-parkinsonian drug receptor signaling. *Neuropharmacology* **54**:1215–1222.
- Lane JR, Powney B, Wise A, Rees S, and Milligan G (2007) Protean agonism at the dopamine D2 receptor: (S)-3-(3-hydroxyphenyl)-*N*-propylpiperidine is an agonist for activation of Go1 but an antagonist/inverse agonist for Gi1, Gi2, and Gi3. *Mol Pharmacol* **71**:1349–1359.
- Lowry OH, Rosebrough NJ, Farr AL, and Randall RJ (1951) Protein measurement with the folin phenol reagent. *J Biol Chem* **193**:265–275.
- Masri B, Salahpour A, Didriksen M, Ghisi V, Beaulieu JM, Gainetdinov RR, and Caron MG (2008) Antagonism of dopamine D2 receptor/ $\beta$ -arrestin 2 interaction is a common property of clinically effective antipsychotics. *Proc Natl Acad Sci USA* **105**:13656–13661.
- Mottola DM, Kilts JD, Lewis MM, Connery HS, Walker QD, Jones SR, Booth RG, Hyslop DK, Piercey M, Wightman RM, Lawler CP, Nichols DE, and Mailman RB (2002) Functional selectivity of dopamine receptor agonists. I. Selective activation of postsynaptic dopamine D2 receptors linked to adenylyl cyclase. *J Pharmacol Exp Ther* **301**:1166–1178.
- Nygaard R, Frimurer TM, Holst B, Rosenkilde MM, and Schwartz TW (2009) Ligand binding and micro-switches in 7TM receptor structures. *Trends Pharmacol Sci* **30**:249–259.
- Oshiro Y, Sato S, Kurahashi N, Tanaka T, Kikuchi T, Tottori K, Uwahodo Y, and Nishi T (1998) Novel antipsychotic agents with dopamine autoreceptor agonist properties: synthesis and pharmacology of 7-[4-(4-phenyl-1-piperazinyl)butoxy]-3,4-dihydro-2(1H)-quinolinone derivatives. *J Med Chem* **41**:658–667.
- Schwartz TW, Frimurer TM, Holst B, Rosenkilde MM, and Elling CE (2006) Molecular mechanism of 7TM receptor activation—a global toggle switch model. *Annu Rev Pharmacol Toxicol* **46**:481–519.
- Spivak CE, Beglan CL, Seidleck BK, Hirshbein LD, Blaschak CJ, Uhl GR, and Surratt CK (1997) Naloxone activation of  $\mu$ -opioid receptors mutated at a histidine residue lining the opioid binding cavity. *Mol Pharmacol* **52**:983–992.
- Swaminath G, Deupi X, Lee TW, Zhu W, Thian FS, Kobilka TS, and Kobilka B (2005) Probing the  $\beta$ 2 adrenoceptor binding site with catechol reveals differences in binding and activation by agonists and partial agonists. *J Biol Chem* **280**:22165–22171.
- Tschammer N, Dörfler M, Hübner H, and Gmeiner P (2010) Engineering a GPCR-ligand pair that simulates the activation of D2L by dopamine. *ACS Chem Neurosci* **1**:25–35.
- Urban JD, Vargas GA, von Zastrow M, and Mailman RB (2007) Aripiprazole has functionally selective actions at dopamine D2 receptor-mediated signaling pathways. *Neuropsychopharmacology* **32**:67–77.
- Wieland K, Zuurmond HM, Krasel C, Ijzerman AP, and Lohse MJ (1996) Involvement of Asn-293 in stereospecific agonist recognition and in activation of the  $\beta$ 2-adrenergic receptor. *Proc Natl Acad Sci USA* **93**:9276–9281.
- Wong YH, Conklin BR, and Bourne HR (1992) Gz-mediated hormonal inhibition of cyclic AMP accumulation. *Science* **255**:339–342.
- Woodward R, Daniell SJ, Strange PG, and Naylor LH (1994) Structural studies on D2 dopamine receptors: mutation of a histidine residue specifically affects the binding of a subgroup of substituted benzamide drugs. *J Neurochem* **62**:1664–1669.
- Yan Z, Feng J, Fienberg AA, and Greengard P (1999) D2 dopamine receptors induce mitogen-activated protein kinase and cAMP response element-binding protein phosphorylation in neurons. *Proc Natl Acad Sci USA* **96**:11607–11612.
- Zuurmond HM, Hessling J, Blüml K, Lohse M, and Ijzerman AP (1999) Study of interaction between agonists and Asn293 in helix VI of human  $\beta$ 2-adrenergic receptor. *Mol Pharmacol* **56**:909–916.

**Address correspondence to:** Prof. Peter Gmeiner, Department of Chemistry and Pharmacy, Friedrich Alexander University, Schuhstraße 19, D-91052 Erlangen, Germany. E-mail: peter.gmeiner@medchem.uni-erlangen.de